hv photonics

IMPACT FACTOR 2.1

CITESCORE 2.6

Communication

Reverse-Engineered Exact Control of Population Transfer in Lossy Nonlinear Three-State Systems

Artur Ishkhanyan

Special Issue

Photonic Integrated Circuits, Sensors, and Instrumentation

Edited by

Dr. Sergey Y. Yurish

MDPI

https://doi.org/10.3390/photonics11111007

photonics

MDPI

Communication

Reverse-Engineered Exact Control of Population Transfer in Lossy Nonlinear Three-State Systems

Artur Ishkhanyan

Institute for Physical Research, Ashtarak 0204, Armenia; aishkhanyan@gmail.com; Tel.: +374-91562258

Abstract: We introduce a reverse-engineered scheme for achieving the precise control of population transfer in nonlinear quantum systems characterized by a 1:2 resonance. This scheme involves the use of two resonant laser pulses that transition from initial and final states to an intermediate level exhibiting irreversible losses. In comparison to alternative techniques, our approach offers computational efficiency advantages. Notably, the analytically defined form of the pump pulse enables tailored control strategies, enhancing robustness against decoherence and imperfections. This flexibility extends to choosing dump pulses and designing time evolution scenarios. These features open doors for practical implementation and scalability in quantum technologies, with potential applications in quantum information processing, quantum computing, and quantum communication.

Keywords: nonlinear three-state systems; population transfer; quantum control; reverse engineering; exact scheme

Citation: Ishkhanyan, A. Reverse-Engineered Exact Control of Population Transfer in Lossy Nonlinear Three-State Systems. *Photonics* **2024**, *11*, 1007. https://doi.org/10.3390/photonics11111007

Received: 30 August 2024
Revised: 29 September 2024
Accepted: 23 October 2024
Published: 25 October 2024

1. Introduction

Effectively manipulating the distribution of particles among their quantum states is a cornerstone of current quantum science and technology research, with continued exploration in this area holding the promise of breakthroughs in various fields [1,2]. This makes it a hot topic with significant ongoing efforts (see, e.g., [3–10] and references therein).

In this paper, we present a novel exact scheme for controlling population transfer in a lossy three-state nonlinear quantum system characterized by a 1:2 resonance through reverse engineering. By reverse engineering, we mean that we start from the desired population dynamics and work backward to determine the appropriate form of the pump pulse, rather than prescribing both the pump and dump pulses from the outset. The technique offers a computationally efficient approach for manipulating quantum systems, allowing tailored control strategies without requiring the same level of computational resources as some alternative methods.

Schematically, achieving population transfer from the initial state to the desired final state involves leveraging an intermediate state, typically characterized by irreversible losses. In this context, "lossy" refers to the assumption that the population in the intermediate state is subject to decay, which can significantly degrade the fidelity of the transfer. By minimizing the occupation of the intermediate state, our scheme enhances overall efficiency and accuracy. Two laser fields are used, each of which resonates with one of the transitions to the intermediate state. Remarkably, the time dynamics of the probability amplitude of the final state can be arbitrarily prescribed. This process exhibits robustness, as the form of the dump pulse can also be freely chosen.

The key control parameter lies in the analytically definable form of the pump pulse. Additionally, it is noteworthy that the freedom in choosing the dump pulse and time evolution scenario for the final state allows for suppressing, via appropriate choice of these functions, the effects of decoherence, experimental imperfections, and non-adiabatic effects, ultimately leading to a higher fidelity process. While minimizing losses in the cintermediate state is a key challenge, the system's nonlinear nature introduces additional complexity

that must also be addressed. Since the system is nonlinear, being characterized by a 1:2 resonance, interactions between states are not proportional to the applied fields. As a result, small changes in control parameters can significantly impact population dynamics. Our reverse-engineered approach handles this nonlinearity effectively, allowing precise control over the population transfer.

Notably, we achieve near-complete population transfer to the target state while minimizing population in the lossy intermediate level through a counterintuitive pulse sequence similar to the case of the STIRAP process. In our approach, the dump pulse is applied before the pump pulse, as in STIRAP, which allows us to effectively suppress the population in the lossy intermediate state. This counterintuitive sequencing is crucial for enhancing fidelity, especially in systems with significant decay.

Beyond the immediate applications in quantum control, this proposed scheme holds the potential for advancements in quantum information processing, quantum computing, and quantum communication. The ability to tailor control strategies with reduced computational demands opens avenues for practical implementation and scalability in quantum technologies. Moreover, the robustness in the face of various challenges positions this scheme as a promising candidate for real-world quantum applications.

2. Derivations

Consider the radiation–matter interaction scheme depicted in Figure 1 (a lambda scheme, though the scheme can also be of a ladder type). Such a scheme is encountered, for example, in the photo- or magneto-association of cold atoms in degenerate quantum gases into diatomic molecules [11–13]. Other examples include photonic systems, quantum dots, and superconducting qubits utilized in diverse fields such as quantum optics ("chi-two" process), quantum information processing, and quantum technology [14–16].

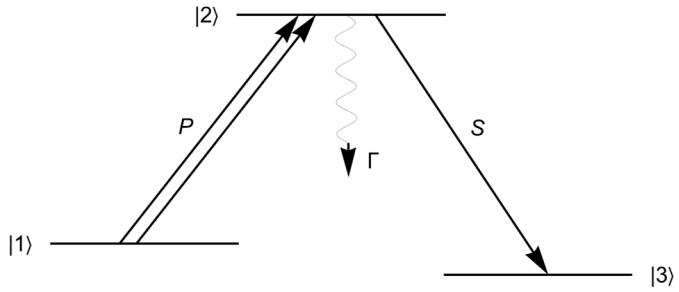

Figure 1. Schematic of a three-state interaction for a 1:2 resonance. *P* (pump) and *S* (dump) fields are resonant with the transitions $|1\rangle \rightarrow |2\rangle$ and $|2\rangle \rightarrow |3\rangle$, respectively. The intermediate state $|2\rangle$ is generally lossy, with a decay rate of Γ.

Thus, we examine a three-state nonlinear quantum system subject to excitation by two monochromatic laser fields: one resonant, with the transition $|1\rangle \rightarrow |2\rangle$, and the other with the transition $|2\rangle \rightarrow |3\rangle$. The direct transition from the first level to the final third one is forbidden, and the intermediate level 2 decays with a rate of Γ. The nonlinearity in the system resembles that of the 1:2 resonance between the quantum states. As quantum mechanics is generally linear, there are several mechanisms through which nonlinearity can arise in quantum systems [17–20]. One well-known example is the Gross–Pitaevskii equation, where nonlinearity emerges from the reduction of the linear many-body problem into a mean-field theory, as seen in the theoretical description of Bose–Einstein condensates.

The 1:2 resonance creates a nonlinear relationship between the population dynamics and the applied fields, even though the two laser fields pump different transitions in the Lambda scheme. The interaction with the intermediate state and the decay further contribute to the nonlinear behavior of the system.

In the rotating-wave approximation, the time-dependent Schrödinger equations that describe the temporal dynamics of such an interaction in the case of one- and two-photon resonances are written as follows:

$$i\hbar\frac{dc_1}{dt} = Pc_2c_1^*, \tag{1}$$

$$i\hbar\frac{dc_2}{dt} = -i\Gamma c_2 + Pc_1^2 + Sc_3, \tag{2}$$

$$i\hbar\frac{dc_3}{dt} = Sc_2, \tag{3}$$

where $c_{1,2,3}$ are the probability amplitudes of the levels indicated by the corresponding indices, c_1^* denotes the complex conjugate of c_1, and $\hbar$ is the reduced Planck constant. The functions $P = P(t)$ (pump) and $S = S(t)$ (dump) are the time-dependent Rabi frequencies of the exciting optical fields. Specifically, P acts on the transition from state $|1\rangle$ to state $|2\rangle$, while S drives the transition from state $|2\rangle$ to state $|3\rangle$. In this analysis, we use dimensionless time for all time-dependent variables. This approach allows us to present the population transfer dynamics in a generalized form, independent of specific system parameters, such as frequency or time units.

The system comprising (1)–(3), which in the lossless case with $\Gamma = 0$ assumes normalization $|c_1|^2 + |c_2|^2 + |c_3|^2 = 1$ can be generated by the following Hamiltonian:

$$H = \frac{P}{2}\left({c_1}^2{c_2}^\dagger + c_2(c_1^\dagger)^2\right) + S\left(c_2{c_3}^\dagger + c_3{c_2}^\dagger\right) - i\hbar\Gamma c_2^\dagger c_2 = H_0 - i\hbar\Gamma c_2^\dagger c_2 \tag{4}$$

Here, H_0 is the Hermitian Hamiltonian describing the 1:2 resonance from state 1 to state 2, and then the transition to state 3. The term $-i\hbar\Gamma c_2^\dagger c_2$ is introduced phenomenologically to simulate the decay of excited state 2 (see, e.g., [17–20]). This Hamiltonian produces operator analogues of Equations (1)–(3) if the Heisenberg equations $i\hbar dc_i/dt = [c_i, H]$ are applied. After deriving the operator equations in the Heisenberg picture, we proceed by treating the operators as c-numbers, as performed, e.g., in Ref. [18] for the case of mean-field equations for the collective two-color photoassociation of a freely interacting gas. This transition allows us to describe the system using probability amplitudes $c_{1,2,3}$ in the Schrödinger picture, where these amplitudes represent the evolution of state probabilities. Note that to meet the applied normalization, one should change $c_1 \to \sqrt{2}c_1$ in the derived equations.

Since amplitude a_1 can be chosen to be real (so that c_3 is also real, and c_2 is imaginary), it is convenient to rewrite system (1) as follows:

$$\frac{i\hbar}{2}\frac{dc_1^2}{dt} = Pc_1^2c_2 \tag{5}$$

$$c_1^2 = \frac{1}{P}\left(i\hbar\frac{dc_2}{dt} + i\Gamma c_2 - Sc_3\right), \tag{6}$$

$$c_2 = \frac{i\hbar}{S}\frac{dc_3}{dt} \tag{7}$$

Substituting Equations (6) and (7) into Equation (5), we obtain a real equation for c_3 [21]:

$$\frac{d}{dt}\ln\left(\hbar^2\frac{d}{dt}\left(\frac{c_3'}{S}\right) + \hbar\Gamma\,\frac{c_3'}{S} + Sc_3\right) = \frac{P'}{P} + \frac{2c_3'}{S}P, \tag{8}$$

where the prime denotes differentiation with respect to time.

In the context of our analysis, an important point to note here is that when we consider an equation with respect to $P(t)$, this presents a first-order ordinary differential equation, which is known as the Bernoulli equation [22,23]:

$$P' + AP + BP^2 = 0 \tag{9}$$

where

$$A(t) = \frac{1}{S}\left(\hbar^2 c_3'' + (\hbar\Gamma - S'/S)c_3' + S^2 c_3\right), \quad B(t) = \frac{2a_3'}{S} \tag{10}$$

This point presents the main step of our approach as compared to most of the alternative approaches applied in the past. Indeed, in most research completed previously, when discussing Equation (8) (or, generally, the governing system (1)–(3)), researchers have typically defined particular forms for the functions $P(t)$ and $S(t)$, developed the solution for the probability amplitudes (either analytically or numerically), and further attempted to optimize the outcomes within the parameter space involved in $P(t)$ and $S(t)$, (see, for example, [24–27]). In contrast, we consider the pump $P(t)$ as an unknown function while assuming the desired form of $c_3(t)$ (as well as the dump $S(t)$) as given. We note that for a two-level case, an approach somewhat akin to ours in ideology has been applied in [28,29].

The integration of Equation (9) is straightforward, yielding an exact result [22,23]:

$$P(t) = \frac{A(t)}{C_0 + \int A(\tau)B(\tau)d\tau}. \tag{11}$$

Here, the integration constant C_0 should be determined from the initial conditions, using Equations (6) and (7). Thus, the pump pulse can be precisely defined for any combination of the dump pulse form $S(t)$ and the time evolution function $c_3(t)$ of the target state's probability amplitude. Finally, we note that in a similar manner, one can track c_1 by adjusting the Rabi frequency $S(t)$ through the corresponding equation for c_1.

Example 1. For

$$c_3 = \frac{a}{2}(1 + \tanh(t)), \quad S = S_0 \mathrm{sech}(t), \tag{12}$$

where a is an arbitrarily variable parameter, we obtain [21]

$$C_0 = -\frac{2S_0}{a} + a\left(S_0 + \frac{\Gamma}{S_0}\right), \tag{13}$$

$$P = \frac{2aS_0\left(S_0^2 e^t - \sinh(t) + \Gamma\cosh(t)\right)}{S_0^2(a^2\sinh(2t) + (a^2-2)\cosh(2t) - 2) + a^2(1 + \Gamma + \Gamma e^{2t})}. \tag{14}$$

The pulse shapes and the occupation probabilities $p_k = |c_k|^2$ and $k = 1, 2, 3$ for parameters $S_0 = 1.5$, $\Gamma = 0.4$, $a = -0.85$, $\hbar = 1$ are shown in Figure 2.

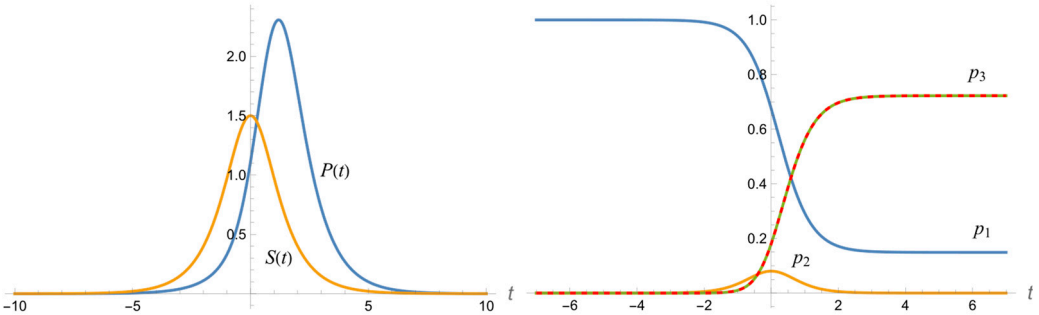

Figure 2. Configuration (12)–(14) (**left panel**) and corresponding occupation probabilities of states $|1\rangle$, $|2\rangle$, and $|3\rangle$ (**right panel**). $S_0 = 1.5$, $\Gamma = 0.4$, $a = -0.85$, $\hbar = 1$.

We note that configuration (12)–(14) is capable of providing almost-complete population transfer to the third level, achieved by setting $a \approx -1$. For a given decay rate of Γ, one should then choose a sufficiently large value of the parameter S_0 to avoid the denominator of the function $P(t)$ from vanishing at a certain point in time (see Equation (14)). This regime is demonstrated in Figure 3 for $a = -0.99$ and $\Gamma = 0.3$. We note that the population

of the lossy intermediate level $|2\rangle$ remains almost zero throughout the entire process, and the pulse sequence in which the dump pulse $S(t)$ precedes the pump pulse $P(t)$ is counterintuitive, as in the case of the STIRAP process [14–16].

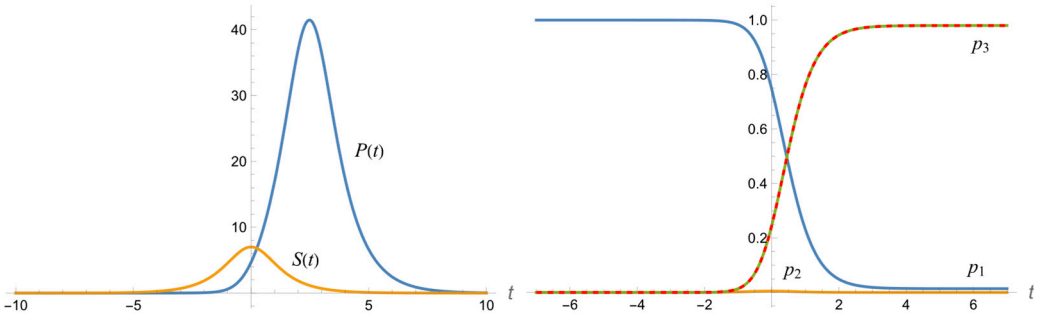

Figure 3. Configuration (12)–(14) (**left panel**) and corresponding occupation probabilities of states $|1\rangle$, $|2\rangle$, and $|3\rangle$ (**right panel**) for parameters $S_0 = 7$, $\Gamma = 0.3$, $a = -0.99$, $\hbar = 1$, which provide almost complete population transfer with $p_3(+\infty) = 0.9801$.

Example 2. In the case when (compare this with (12))

$$c_3 = \frac{a}{2}\Big(1 + \tanh(t) + \mathrm{sech}^2(t)\Big) \text{and } S = S_0 \mathrm{sech}(t), \tag{15}$$

the integration constant is found to be [21]

$$C_0 = \frac{a^2}{6}\left(3 + \frac{7\Gamma}{S_0^2}\right) - 1, \tag{16}$$

and the resulting occupation probabilities are shown in Figure 4.

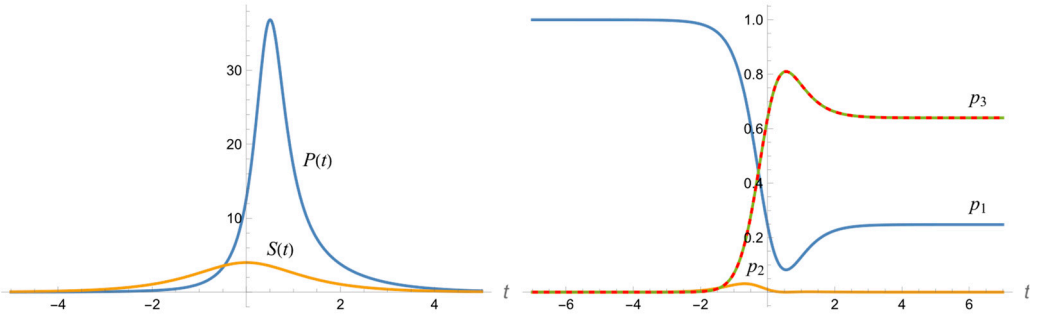

Figure 4. Configurations (15) and (16) (**left panel**) and corresponding occupation probabilities of states $|1\rangle$, $|2\rangle$, and $|3\rangle$ (**right panel**). $S_0 = 4$, $\Gamma = 1.2$, $a = -0.8$, $\hbar = 1$.

3. Conclusions

This paper introduces an exact scheme for controlling population transfer in a lossy three-state nonlinear quantum system through reverse engineering. The assumed nonlinearity is local and resembles a 1:2 resonance. The key development lies in the precise definition of the pump pulse, enabling tailored control strategies with reduced computational demands compared to alternative methods.

The derivations section details the radiation–matter interaction scheme, providing a clear foundation. The time-dependent Schrödinger equations derived in the rotating-wave approximation offer a comprehensive description of the system's behavior under the influence of two monochromatic laser fields. The re-parametrization of the system in terms of real amplitudes simplifies the equations, facilitating a more manageable and insightful analysis. The integration of the first-order differential equation for the probability amplitude of the final state underscores the effectiveness of the proposed scheme. The obtained result provides a means to precisely define the pump pulse for arbitrary

combinations of the dump pulse form and the time evolution function of the target state's probability amplitude.

The robustness in the face of challenges, such as decoherence, experimental imperfections, and non-adiabatic effects, positions this scheme as a promising candidate for practical implementation in real-world quantum technologies, such as quantum information processing, quantum computing, and quantum communication. Two illustrative examples showcase the dynamics of the system under the proposed scheme, providing insight into the occupation probabilities for different configurations.

In conclusion, the paper contributes to the field of quantum control by presenting a novel reverse-engineered approach to population transfer in three-state nonlinear quantum systems. The presented exact scheme, along with its potential applications and robustness, opens new avenues for advancements in quantum science and technology. Notably, the achieved high-fidelity population transfer to the target state while minimizing the population in the lossy intermediate level through a counterintuitive pulse sequence, similar to the case of the STIRAP process, demonstrates the potential of this approach for practical applications.

Funding: This research was funded by the Armenian State Committee of Science, grant number 21AG-1C064.

Data Availability Statement: Data sharing is not applicable to this article.

Acknowledgments: This article is a revised and expanded version of a paper entitled "Precise control of population transfer in nonlinear lambda systems through reverse engineering", which was presented at the 7th International Conference on Optics, Photonics and Lasers (OPAL'2024), Palma de Mallorca, Baleares, Spain, 15–17 May 2024.

Conflicts of Interest: The author declares no conflicts of interest.

References

1. Glaser, S.J.; Boscain, U.; Calarco, T.; Koch, C.P.; Kockenberger, W.; Kosloff, R.; Kuprov, I.; Luy, B.; Schirmer, S.; Schulte-Herbrüggen, T.; et al. Training Schrödinger's cat: Quantum optimal control. Strategic report on current status, visions, and goals for research in Europe. *Eur. Phys. J. D* **2015**, *69*, 279. [CrossRef]
2. Koch, C.P.; Boscain, U.; Calarco, T.; Dirr, G.; Filipp, S.; Glaser, S.J.; Kosloff, R.; Montangero, S.; Schulte-Herbrüggen, T.; Sugny, D.; et al. Quantum optimal control in quantum technologies. Strategic report on current status, visions, and goals for research in Europe. *EPJ Quantum Technol.* **2022**, *9*, 19. [CrossRef]
3. Ivanov, S.S.; Torosov, B.T.; Vitanov, N.V. High-Fidelity Quantum Control by Polychromatic Pulse Trains. *Phys. Rev. Lett.* **2022**, *129*, 240505. [CrossRef]
4. Guéry-Odelin, D.; Ruschhaupt, A.; Kiely, A.; Torrontegui, E.; Martínez-Garaot, S.; Muga, J.G. Shortcuts to adiabaticity: Concepts, methods, and applications. *Rev. Mod. Phys.* **2019**, *91*, 045001. [CrossRef]
5. Petiziol, F.; Arimondo, E.; Giannelli, L.; Mintert, F.; Wimberger, S. Optimized three-level quantum transfers based on frequency-modulated optical excitations. *Sci. Rep.* **2020**, *10*, 2185. [CrossRef] [PubMed]
6. Zhu, J.; Chen, X. Fast-forward scaling of atom-molecule conversion in Bose-Einstein condensates. *Phys. Rev. A* **2021**, *103*, 023307. [CrossRef]
7. Vepsäläinen, A.; Danilin, S.; Paraoanu, G.S. Superadiabatic population transfer in a three-level superconducting circuit. *Sci. Adv.* **2019**, *5*, eaau5999. [CrossRef]
8. Dorier, V.; Gevorgyan, M.; Ishkhanyan, A.; Leroy, C.; Jauslin, H.R.; Guérin, S. Nonlinear stimulated Raman exact passage by resonance-locked inverse engineering. *Phys. Rev. Lett.* **2017**, *119*, 243902. [CrossRef]
9. Laforgue, X.; Chen, X.; Guérin, S. Robust stimulated Raman exact passage using shaped pulses. *Phys. Rev. A* **2019**, *100*, 023415. [CrossRef]
10. Zhu, J.J.; Liu, K.; Chen, X.; Guerin, S. Optimal control and ultimate bounds of 1:2 nonlinear quantum systems. *Phys. Rev. A* **2023**, *108*, 042610. [CrossRef]
11. Mackie, M.; Kowalski, R.; Javanainen, J. Bose-stimulated Raman adiabatic passage in photoassociation. *Phys. Rev. Lett.* **2000**, *84*, 3803. [CrossRef]
12. Drummond, P.D.; Kheruntsyan, K.V.; Heinzen, D.J.; Wynar, R.H. Stimulated Raman adiabatic passage from an atomic to a molecular Bose-Einstein condensate. *Phys. Rev. A* **2002**, *65*, 063619. [CrossRef]
13. Ling, H.Y.; Pu, H.; Seaman, B. Creating a stable molecular condensate using a generalized Raman adiabatic passage scheme. *Phys. Rev. Lett.* **2004**, *93*, 250403. [CrossRef] [PubMed]

14. Bergmann, K.; Vitanov, N.V.; Shore, B.W.; Bergmann, K. Perspective: Stimulated Raman adiabatic passage: The status after 25 years. *J. Chem. Phys.* **2015**, *142*, 170901. [CrossRef] [PubMed]
15. Vitanov, N.V.; Rangelov, A.A.; Shore, B.; Bergmann, K. Stimulated Raman adiabatic passage in physics, chemistry, and beyond. *Rev. Mod. Phys.* **2017**, *89*, 015006. [CrossRef]
16. Bergmann, K.; Nägerl, H.C.; Panda, C.; Gabrielse, G.; Miloglyadov, E.; Quack, M.; Quack, M.; Seyfang, G.; Wichmann, G.; Ospelkaus, S.; et al. Roadmap on STIRAP applications. *J. Phys. B* **2019**, *52*, 202001. [CrossRef]
17. Olsen, M.K.; Plimak, L.I.; Kruglov, V.I.; Hope, J.J.; Drummond, P.D.; Collett, M.J. Dynamics of trapped Bose-Einstein condensates: Beyond the mean-field. *Laser Phys.* **2002**, *12*, 21–36.
18. Mackie, M.; Härkönen, K.; Collin, A.; Suominen, K.-A.; Javanainen, J. Improved efficiency of stimulated Raman adiabatic passage in photoassociation of a Bose-Einstein condensate. *Phys. Rev. A* **2004**, *70*, 013614. [CrossRef]
19. Javanainen, J.; Mackie, M. Coherent photoassociation of a Bose-Einstein condensate. *Phys. Rev. A* **1999**, *59*, R3186. [CrossRef]
20. Kheruntsyan, K.V.; Drummond, P.D. Multidimensional parametric quantum solitons. *Phys. Rev. A* **1998**, *58*, R2676. [CrossRef]
21. Ishkhanyan, A.M. Precise control of population transfer in nonlinear lambda systems through reverse engineering. In Proceedings of the 7th International Conference on Optics, Photonics and Lasers (OPAL' 2024), Islands, Spain, 15–17 May 2024; pp. 187–188.
22. Zwillinger, D. *Handbook of Differential Equations*, 3rd ed.; Academic Press: Boston, MA, USA, 1997.
23. Zaitsev, V.F.; Polyanin, A.D. *Handbook of Ordinary Differential Equations: Exact Solutions, Methods, and Problems*, 3rd ed.; Chapman and Hall/CRC: Boca Raton, FL, USA, 2007.
24. Shi, Z.; Zhang, C.; Ran, D.; Xia, Y.; Ianconescu, R.; Friedman, A.; Yi, X.X.; Zheng, S. Composite pulses for high fidelity population transfer in three-level systems. *New J. Phys.* **2022**, *24*, 023014. [CrossRef]
25. Guérin, S.; Gevorgyan, M.; Leroy, C.; Jauslin, H.R.; Ishkhanyan, A. Efficient adiabatic tracking of driven quantum nonlinear systems. *Phys. Rev. A* **2013**, *88*, 063622. [CrossRef]
26. Shirkhanghah, N.; Saadati-Niari, M. Nonlinear fractional stimulated Raman exact passage in three-level λ systems. *Rev. Mex. Física* **2020**, *66*, 344–351. [CrossRef]
27. Chen, X.; Ban, Y.; Hegerfeldt, G.C. Time-optimal quantum control of nonlinear two-level systems. *Phys. Rev. A* **2016**, *94*, 023624. [CrossRef]
28. Messina, A.; Nakazato, H. Analytically solvable Hamiltonians for quantum two-level systems and their dynamics. *J. Phys. A* **2014**, *47*, 445302. [CrossRef]
29. Barnes, E.; Das Sarma, S. Analytically solvable driven time-dependent two-level quantum systems. *Phys. Rev. Lett.* **2012**, *109*, 060401. [CrossRef]